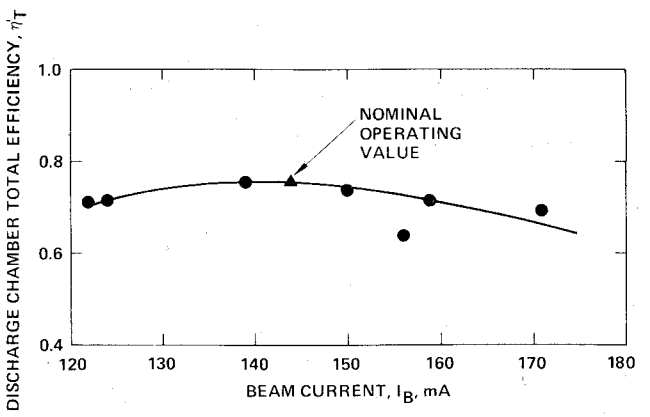


**Fig. 6 Discharge-chamber total efficiency $\eta_T'$ as a function of beam current $I_B$ for 2-mlb optimized DCM.**

confirmed by obtaining a mercury flowrate measurement from volumetric displacement of a liquid column over a 1-h period. Discharge-chamber performance for a given configuration was characterized for operation over the range in discharge voltage $37V \leq V_D \leq 40V$ and over a range of discharge current values (determined by discharge stability) with $V_D = 40V$.

The basic geometry of the 2-mlb DCM has also been tentatively chosen for operation at the thrust level $T = 4$ mlb with performance modifications resulting mainly from a change in the method of delivery of mercury vapor to the discharge chamber. In the present 4-mlb DCM configuration, approximately 30% of the mercury-vapor flow is transmitted through a diffuser plate located between the end of the discharge chamber and the base of the cathode-cup polepiece. Thus far, no optimization of discharge-chamber size or magnetic field shape or intensity has been attempted and only preliminary optimization has been attempted with regard to cathode position or in selection of electron baffle size and diffuser plate design.

## DCM Performance

The results of the 0.5-mlb DCM optimization tests are shown in Figs. 3 and 4. In Fig. 3, the discharge specific energy $\epsilon_I$ is plotted as a function of discharge-chamber propellant utilization efficiency $\eta_{Hg}'$. The utilization efficiency reaches a maximum value of $\eta_{Hg}' \approx 80\%$. In Fig. 4, the discharge-chamber total efficiency $\eta_T'$ is shown as a function of a beam current $I_B$; discharge-chamber total efficiency reaches a maximum value for beam currents in the range $35\,mA \leq I_B \leq 40mA$.

The results of the 2-mlb DCM optimization tests are shown in Figs. 5 and 6. Figure 5 shows that discharge-chamber propellant utilization reaches a maximum of 93%; Figure 6 shows that total discharge-chamber efficiency $\eta_T'$ varies only slightly over the range of beam-current values recorded.

Table 2 summarizes performance of the three DCM's in their final configurations with ion-machined accel apertures, Performance of the l-mlb EMT with chemically machined accel electrode is also included for reference. For the 0.5-mlb DCM with the ion-machined apertures, discharge-chamber propellant utilization is significantly higher than the values obtained with photo-etched apertures shown in Fig. 3. This difference is not as pronounced for the 2-mlb DCM, however, since the aperture diameters of the 2-mlb DCM ion-machined optics were nearly identical to the 2-mlb DCM photo-etched apertures.

## Conclusions

An efficient method has been developed for scaling the thrust level of an ion thruster by use of separate discharge-chamber modules while retaining all critical subassemblies of the basic system design.[1] This scaling has been demonstrated in the range of thrust levels from 0.5-4.0 mlb.

## Acknowledgment

This work was supported in part by the NASA Lewis Research Center under NASA Contract NAS 3-19691. Technical development was carried out at Hughes Research Laboratories in cooperation with the Small Thruster Section of the Electric Propulsion Branch of NASA Lewis Research Center.

## References

[1] Hyman, J. Jr. and Dulgeroff, C. R., "Modularized Ion Thruster," Hughes Research Labs., Malibu, Calif., Final Rept. on NASA Contract NAS 3-19691 NASA CR134667, 1976.

[2] Herron, B. G., Hyman, J. Jr., and Hopper, D. J., "8-cm Engineering Model Thruster Development," AIAA Paper 76-1058, AIAA 12th Electric Propulsion Conference, Key Biscayne, Fla., Nov. 1976.

[3] Free, B. A., "Electric Propulsion Technology Status and Development Plans: Commercial Satellite Programs," AIAA Paper 73-1145, AIAA 10th Electric Propulsion Conference, Lake Tahoe, Nev., Oct.-Nov. 1973.

[4] Mitchell, D. H. and Huberman, M. N., "Ion Propulsion for North-South Stationkeeping of Communication Satellites," AIAA Paper 76-290, AIAA/CASI 6th Coomunications Satellite Systems Conference, Montreal, Can., April 1976.

[5] Hyman, J. Jr. and Poeschel, R. L., "Satellite Control Mercury Ion Thruster," AIAA Paper 73-1132, AIAA 10th Electric Propulsion Conference, Lake Tahoe, Nev., Oct-Nov. 1973.

[6] Hudson, W. R., "Auxiliary Propulsion Thruster Performance with Ion-Machined Accelerator Grids," AIAA Paper 75-425, AIAA 11th Electric Propulsion Conference, New Orleans, La. March 1975.

# Approximate Velocity of Bodies Powered by Cold-Gas Thrusters with Small Propellant Mass

M. D. Bennett*
*Sandia Laboratories, Albuquerque, N. Mex.*

## Nomenclature

| | |
|---|---|
| $b$ | = mass-fraction parameter $= \lambda/(1-\lambda)$ |
| $c_i$ | = initial speed of sound in propellant gas, m/s |
| $I_s$ | = thruster specific impulse, m/s |
| $k$ | = specific-heats parameter $= 2/(\gamma-1)$ |
| $m_f$ | = vehicle final mass, kg |
| $m_i$ | = vehicle initial mass, including propellant gas, kg |
| $R$ | = gas constant, J/kg − K |
| $T_i$ | = gas initial temperature, K |
| $v_{max}$ | = vehicle terminal velocity, m/s |
| $\gamma$ | = ratio of specific heats of ideal gas |
| $\zeta$ | = specific-heats factor $= (\gamma+1)/(\gamma-1)$ |
| $\theta$ | = specific-heats term $= [2/(\gamma+1)][2/(\gamma-1)]^{1/2}$ |
| $\lambda$ | = vehicle mass fraction $= m_f/m_i$ |

## Introduction

SEVERAL previous investigations of the translational motion of a missile discharging an inert propulsive gas from a thermally insulated tank involved an integral equation

Received Jan. 19, 1978. 

Index categories: Missile Systems; Fuels and Propellants, Properties of.

*Member of Technical Staff, Aerodynamics Department. Associate Fellow AIAA.

that expressed the ideal velocity attained by the body.[1-3] The analytical solution pertaining the general case of arbitrary specific-heats ratio $\gamma$ had the form of an infinite geometric series. However, for the category of fluids that yield integer values of the function $f(\gamma)=2/(\gamma-1)$, which describes the molecular degrees of freedom in an ideal gas, a relatively compact formula evolved. Ultimately, the special solution was expanded in detail for the monotomic and diatomic gases.[1,2] For the polyatomic gases, resort was made to numerical solution because the governing analytical expression becomes somewhat unwieldy with the many-degrees-of-freedom gases.[3]

In the present discussion, an approximate solution of the velocity equation is developed to provide a more convenient means of assessing the effects of various design parameters. The approximation applies when the working fluid comprises a small part of the total mass, which is the usual situation with current designs of cold-gas thruster systems. It displays particularly good accuracy in the case of the polyatomic gases, where numerical solution was formerly used.

## Solution of Velocity Equation for Small Propellant Mass

The integral equation that describes the ideal velocity imparted to a missile due to releasing a pressurized gas from a thermally insulated tank was previously found to be (see Eq. (3), Ref. 2)

$$v_{\max}=k^{3/2}(1-\mathcal{I})c_i \tag{1}$$

where $k$ denotes, in effect, the molecular degrees of freedom of the working fluid; $c_i=\sqrt{\gamma RT_i}$ represents the fluid's initial speed of sound; and the dimensionless parameter $\mathcal{I}$ is

$$\mathcal{I}=b^{1/k}\int_0^{(1/b)^{1/k}}\frac{d\xi}{1+\xi^k} \tag{2}$$

This integral has a known solution[1,2] for integer values of $k$, but the terms of the resulting expression become increasingly cumbersome, as well as more numerous, if $k$ becomes large, which is the circumstance with polyatomic gases.[3]

A general solution of the equation that describes the vacuum velocity of the variable-mass body may be obtained by writing the integrand of Eq. (2) as a binominal series, and integrating each term separately. With that procedure, the velocity factor $(1-\mathcal{I})$ becomes

$$1-\mathcal{I}=\frac{1/b}{1+k}-\frac{(1/b)^2}{1+2k}+\frac{(1/b)^3}{1+3k}-\frac{(1/b)^4}{1+4k}+\ldots \tag{3}$$

provided that the propellant mass does not exceed one-half the total mass, i.e., provided $1/b=(1-\lambda)/\lambda<1$, which corresponds to $\lambda=m_f/m_i>\frac{1}{2}$.

Equation (3) may be rearranged in the form of a logarithmic parameter plus a residual series:

$$1-\mathcal{I}=\left(\frac{1}{1+k}\right)\left\{-\ell n(\lambda)+\sum_{j=1}^{\infty}(-1)^j\left(\frac{j}{j+1}\right)\times\left[\frac{1}{1+(j+1)k}\right]\left(\frac{1-\lambda}{\lambda}\right)^{j+1}\right\} \tag{4}$$

The summed function in the above formula is a rapidly converging series with terms of alternating sign, and the error due to truncating the $j$th and higher order terms is less than

$$\left|\left(\frac{j}{j+1}\right)\left[\frac{1}{1+(j+1)k}\right]\left(\frac{1-\lambda}{\lambda}\right)^{j+1}\right|$$

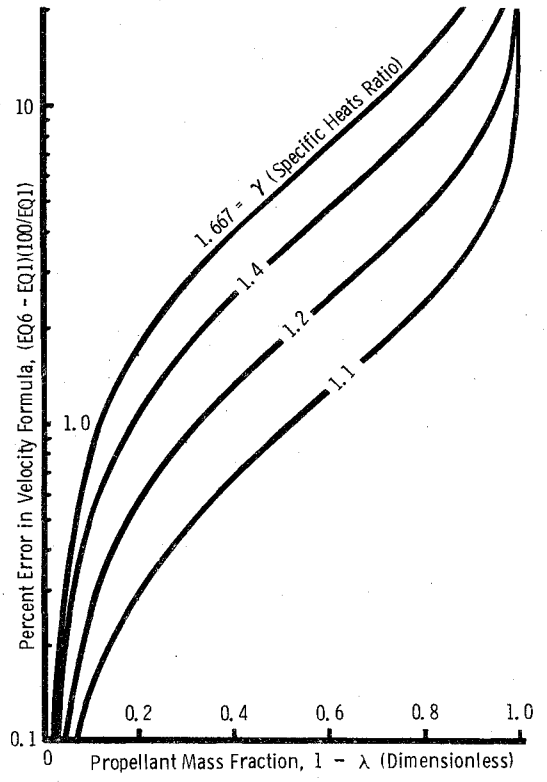


**Fig. 1 Comparison of approximate velocity formula with integral equation for various working fluids.**

If the propellant mass is initially small ($\lambda\to 1$), the summed term in Eq. (4) approaches zero. In that event, the asymptotic solution for the velocity factor becomes $(1-\mathcal{I})=(1+k)^{-1}\ell n(1/\lambda)$. Consequently, the approximate solution of the integral equation reduces to

$$v_{\max}\cong[k^{3/2}/(1+k)]c_i\ell n(1/\lambda) \tag{5}$$

Written in terms of the ratio of specific heats, the alternative form of Eq. (5) is

$$v_{\max}\cong[2/(\gamma+1)]\sqrt{2\gamma RT_i/(\gamma-1)}\,\ell n(1/\lambda) \tag{6}$$

Equation (6) provides a simple means of estimating the effects of the type and quantity of propulsive fluid, and the initial temperature.

## Approximate Velocity in Terms of Specific Impulse

The velocity may be expressed also as a function of the thruster impulse. It has been shown (Eq. (7), Ref. 1) that the impulse $I$ produced by isentropically discharging the gaseous contents of a tank through an infinite area ratio nozzle into a vacuum is $I=\theta m_i c_i$, where $m_i$ represents the gas initial mass and the premultiplier $\theta$ is a known function of the specific heats ratio. The corresponding specific impulse $I_s$ is

$$I_s=\theta c_i \tag{7}$$

According to an elementary molecular model,[4] the ratio of specific heats is related to the internal degrees of freedom by the formula $\gamma=(k+2)/k$. When this formula is substituted into Eq. (7), the specific impulse takes the form

$$I_s=[k^{3/2}/(1+k)]c_i \tag{8}$$

Since the right-hand side of Eq. (8) is the same as the coefficient of the logarithmic function in Eq. (6), the approximate

equation of velocity reduces to

$$V_{max} \cong I_s \ell n(1/\lambda) \quad (9)$$

Equation (9) is identical, except for the "approximately equal" notation, to the well-known formula that gives the ideal velocity attained by a conventional rocket in a gravitationless vacuum,† the derivation of which assumes that the exhaust velocity and mass flow rate remain constant. Both of these items, however, are varying in the case of the cold-gas thruster.

### Accuracy of Approximation

By comparing Eqs. (1) and (5), it may be seen that the terminal velocity, according to the approximate formula, is slightly overestimated. The maximum percentage error occurs with thrusters using the monatomic gases ($k = 3$ or $\gamma = 1.667$), and amounts to about 5% in the extreme case of $\lambda = \frac{1}{2}$. As indicated in Fig. 1, the difference between the two equations decreases as $k$ or $\lambda$ grows large, such that the error in any situation does not exceed 1% for propellant mass fractions ranging up to 10%.

†See, for example, Ref. 5.

It may be concluded that for the class of cold-gas thrusters containing small propellant mass, the approximate velocity equation closely represents the integral equation of ideal velocity. The abbreviated formula permits the effect of various design factors to be readily determined.

### Acknowledgment

This work was supported by the U.S. Department of Energy.

### References

[1] Bennett, M. D., "Velocity of Bodies Powered by Rapidly Discharged Cold-Gas Thrusters," *Journal of Spacecraft and Rockets*, Vol. 12, April 1975, pp. 254-256.

[2] Bennett, M. D., "Velocity of Bodies Powered by Diatomic Cold-Gas Thrusters," *Journal of Spacecraft and Rockets*, Vol. 13, Oct. 1976, pp. 624-626.

[3] Bennett, M. D., "Velocity of Bodies Powered by Polyatomic Cold-Gas Thrusters," *Journal of Spacecraft and Rockets*, Vol. 14, June 1977, pp. 379-381.

[4] Zucrow, M. I. and Hoffman, J. D., *Gas Dynamics*, Vol. 1, Wiley, New York, 1976, p. 44.

[5] Sutton, G. P., *Rocket Propulsion Elements*, 3rd Ed., Wiley, New York, 1963, p. 125.

# Technical Comments

## Comment on "A Re-Entry Control Effectiveness Methodology for the Space Shuttle Orbiter"

Lars E. Ericsson and J. Peter Reding
*Lockheed Missiles & Space Company, Inc., Sunnyvale, Calif.*

IKAWA, in his strip-analysis of the control characteristics of the Space Shuttle Orbiter,[1] draws conclusions that easily can be interpreted to mean that there are no significant three-dimensional flow effects in the separated flow region generated by windward side control deflection. This is a gross misinterpretation of the experimental results.

Even when the inviscid flow is axisymmetric, large-scale three-dimensional flow characteristics are observed in the separated flow region caused by a compression corner.[2] Consequently, the "nearly two-dimensional" attached flow characteristics existing on the windward side of the Orbiter, deduced from the flow picture in Fig. 2 of Ref. 1, and also demonstrated by the theoretical and experimental investigations by Adams et al.,[3] does not imply that the control-induced separated flow region also will be "nearly two-dimensional" in character. Ikawa admits as much but concludes that because the control hinge line is unswept in his case the gross effects on the Space Shuttle Orbiter control surface effectiveness can be analyzed by his strip-theory approach with reasonable accuracy "even though the microscopic flow field detail may be highly three-dimensional." If the three-dimensional effects truely were microscopic, this would be true. However, Whitehead and Keyes[4] tested a control with straight unswept hinge line on a delta wing and found the separated flow region to be highly three-dimensional, containing large-scale vortices. These separated flow characteristics were obtained with natural boundary-layer transition occurring well inboard of the leading edge. When roughness was applied near the leading edge, causing the transition to move closer to the leading edge, a more regular separated flow region was obtained. Even in the more regular separated flow region obtained with roughness, the effects of spanwise flow were found to be large. The effect of this spanwise flow is to shrink the separated flow extent[4] and to decrease the pressure in the separated flow region.[5] The results presented by Marvin et al.[6] show such three-dimensional flow effects even for control-induced turbulent flow separation.‡

Ikawa[1] acknowledges that spanwise flow tends to reduce the separated flow region. This "shrinking" of the separated flow region due to spanwise flow will by itself, without considering any pressure changes, change the separation-induced loads. The sketch in Fig. 1 illustrates how the decrease of the extent of the pressure plateau causes the separation-induced normal force to lose the forward component $\Delta C_{N1}$. The earlier reattachment on the flap adds the aft normal force component $\Delta C_{N2}$. For a certain control geometry it is possible that the two force components could cancel each other, i.e., $\Delta C_{N2} - \Delta C_{N1} = 0$. However, in this case the pitching moment would be decreased by the stabilizing component $\Delta C_m = -\Delta\xi \cdot \Delta C_N$, where $\Delta C_N = \Delta C_{N1} = \Delta C_{N2}$. Ikawa's data display precisely these characteristics (Fig. 8 of Ref. 1). That is, the measured control-induced normal force is essentially in agreement with prediction, whereas the measured control-induced pitching moment is underpredicted.§ Thus, a comparison between strip-theory and experiment based upon gross normal force

Received Dec. 12, 1977. 

Index categories: Supersonic and Hypersonic Flow; Jets, Wakes, and Viscid-Inviscid Flow Interactions.

*Consulting Engineer. Associate Fellow AIAA.

†Research Specialist. Member AIAA.

‡The 22 deg swept hinge line may have contributed somewhat to the three-dimensionality in their case.

§This is clearly the case for $\alpha = 40$ deg, whereas the experimental data scatter extends across predictions for $\alpha = 30$ and $\alpha = 20$ deg.